# Sensitivity of ARGO-YBJ to different composition models in the energy range 10 ÷ 500 TeV

M. Iacovacci, T. Di Girolamo, G. Di Sciascio, S. Mastroianni and L. Saggese

Dip. di Fisica - Università di Napoli and INFN sez. di Napoli, Italy

On behalf of the ARGO-YBJ Collaboration (*)

The ARGO-YBJ experiment is currently under construction at the Yangbajing Cosmic Ray Laboratory (4300 m a.s.l.). The detector consists of a central *carpet*, $74 \times 78$ m$^2$, made of a single layer of Resistive Plate Counters (RPCs), and surrounded by a partially instrumented guard ring for a total instrumented area of about 6700 m$^2$. The digital read-out, performed by means of pick-up electrodes $6.7 \times 62$ cm$^2$ (*strip*), allows to measure the charged particle number of small size air showers. The technique of counting the number of fired strips on the ARGO carpet corresponds to operate in the 10÷500 TeV energy region where both direct and indirect measurements on the primary cosmic radiation have been performed. Many composition models have been proposed by different experiments. In this work we discuss the ability of the ARGO detector to discriminate among some models.

## 1. Introduction

The energy spectrum of cosmic rays is well described by a power law over several decades of energy, before and after the so called knee region, $10^{15} \div 10^{16}$ eV, where the slope changes. Despite of many conjectures and efforts, the origin of this steepening, observed in air shower data, is still obscure. At present it is not clear if this phenomenon reflects a limit in the acceleration mechanism or results from propagation and diffusion of cosmic rays in the galactic environment. Other mechanisms like interactions with background particles (neutrinos in the galactic halo, background photons) or new interactions in the atmosphere seem to be less favorite [1]. Although measurements have become more and more accurate, nevertheless the comparison of existing data makes evident a substantial disagreement between the primary cosmic ray composition models provided by different experiments. As pointed out by many authors the statistical accuracy is no more the main problem, instead the accuracy of the simulation programs is stressed and the need for cross section measurements at a much better accuracy than available at moment, at least in the kinematical region of interest to cosmic ray experiments. This is true both for direct and indirect measurements. As

an example, the proton spectrum measured by TIBET ASγ [2] changes its slope around 100 TeV, KASCADE [3] data suggest instead a steepening at about 2 PeV while data collected by the balloon-born experiment RUNJOB [4] do not exhibit any spectral break up to 500 TeV.

The problem of an "absolute" normalization exists and what the people do is to match direct and indirect measurements. In this respect, ARGO-YBJ offers a unique opportunity because of its ability to operate down to few TeV by measuring small size air showers (strip or digital read-out) and up to the PeV region by measuring the RPC charge (analog read-out).

In this paper we discuss the ARGO sensitivity to discriminate between different models of primary cosmic ray composition in the 10÷500 TeV energy range by exploiting the digital read-out of the detector. First we will describe the detector, then the calculation method. It follows a description of the composition models used to estimate the strip multiplicity distribution in ARGO. The results of the calculation will be then discussed and finally some conclusions will be drawn.

(*) cfr ref. [5] for the Collaboration list.

## 2. The ARGO-YBJ detector and the digital read-out

The ARGO-YBJ detector [5] is located in Tibet (P.R.China) at the Yangbajing High Altitude Cosmic Ray Laboratory (30.11° N, 90.53° E, 4300 m a.s.l., 606 $g/cm^2$ ). It consists (Fig.1) of a single layer of RPCs operated in streamer mode [6], $74 \times 78$ $m^2$ wide, with an active area of 92%, surrounded by a guard ring. The signals from each RPC are picked-up with 80 read-out strips, 6.7 cm wide and 62 cm long, with an average density of 22 strips/ $m^2$ for a total of 124800 strips in the central carpet. The FAST-OR of 8 contiguous strips defines a logical unit called PAD (10 PADs for each RPC) whose signal is used for timing and trigger purpose. The detector is divided in units of 12 RPCs (CLUSTER) whose read-out is made by a Local Station (LS) which represents the DAQ elemental unit.

The two main features of ARGO-YBJ, namely operation at high altitude and full coverage, make it unique. Indeed owing to its low energy threshold $E_{th}$ (300÷500 GeV), it realizes a "bridge" between direct and indirect measurements; furthermore it provides a very detailed representation of the shower front both in space and time (high granularity and $\sigma_t \approx 1$ ns).
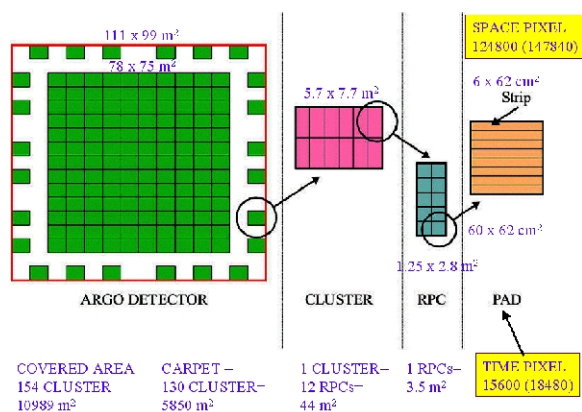


Fig. 1. Schematic view of the ARGO-YBJ detector

A simulation [7] has been carried out by means of the CORSIKA/QGSjet code [8] in order to study the energy dependence of the number of fired strips for

quasi-vertical showers (zenith angle $\theta < 15°$) with core in a fiducial area ($A_f$) of about 260 $m^2$ at the center of the carpet ($2 \times 3$ CLUSTERs). An average efficiency of 95% and an average strip multiplicity m =1 .2 strip/particle have been taken into account. The average strip size, $N_s$, is compared in Fig.2 to the total size and to the size sampled by the central carpet ("truncated size") for proton induced showers. Fig. 2 clearly shows that the digital response of the detector can be used to study the primary spectrum up to energies of a few hundreds of TeV. In order to extend the dynamic range a charge read-out has been implemented by instrumenting each RPC with two large size pads $140 \times 125$ $cm^2$ each ("Big Pad") [9].
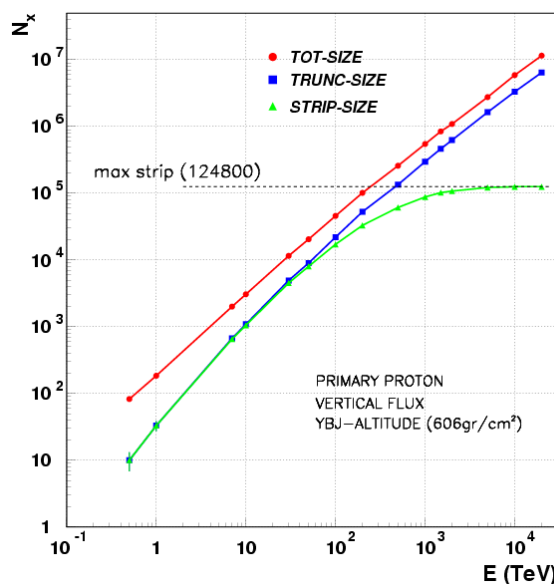


Fig. 2. Average strip size compared to the total size and the size sampled by the ARGO carpet -truncated size - .

## 3. The strip size spectrum

In order to study the capability of the ARGO detector, operated in digital mode, to discriminate between different composition models of the primary radiation, the strip multiplicity spectrum has to be calculated according to each model. The method used in this work is semi-analytical. If $N_s$ is the strip multiplicity, $J_A(N_s)$ the multiplicity

spectrum provided by an elemental nucleus of mass A and $J_{all}(N_s)$ the multiplicity spectrum summed over all the elemental nuclei, then

$$J_{all}(N_s) = \sum_A J_A(N_s)$$

where $J_A(N_s)$ is given by

$$J_A(N_s) = \varepsilon_A(N_s) \int J_A(E) P_A(E, N_s) dE$$

In this formula appear $J_A(E)$, which is given by the composition model, and the probability $P_A(E, N_s)$ that an elemental nucleus of mass A produces a multiplicity strip $N_s$ on the detector, provided it has been detected. The detection efficiency is $\varepsilon_A(N_s)$. Both $P_A(E, N_s)$ and $\varepsilon_A(N_s)$ have been calculated by Monte Carlo.

### $J_A(E)$ : Composition Models

The following models for the primary composition have been considered: JACEE [10]; RUNJOB [4]; TIBET ASγ [2] and the model proposed by J.R. Horandel [11] to fit the world data both from direct and indirect measurements. The first two come from balloon-born experiments which provided data up to hundreds of TeV, although they suffer from statistics for E >100 TeV. TIBET ASγ provided data above 300 TeV. There is no special reason for selecting the above mentioned models unless the particular energy range we want to study, which is a "bridge" region between direct and indirect measurements, therefore we need data from direct measurements at the highest energies along with data from air shower measurements, in the widest energy range.

The JACEE model is shown in Fig. 3a. There $f_A(E) = J_A(E) E^{2.5}$ is reported, where $J_A(E)$ is the element spectrum as function of the nucleus energy. The maximum energy ranges in 800÷1000 TeV depending on the nuclear element. The proton and alpha spectra are consistent with a single power law over the entire energy range. The possible break in the proton spectrum, initially claimed [12], is neither confirmed nor excluded [10, 13], the conclusion being that a significantly better statistics is required in order to address the question of a proton spectral break. For heavier elements, that means CNO and NeMgSi groups and the Fe group, the statistics is much poorer (25-30 events per group). For protons

and alphas the fit parameters provided by the collaboration have been adopted, while we have fitted ourselves the spectra of the other groups with a single power law; the points above $10^{15}$ eV have not been included in the fit.
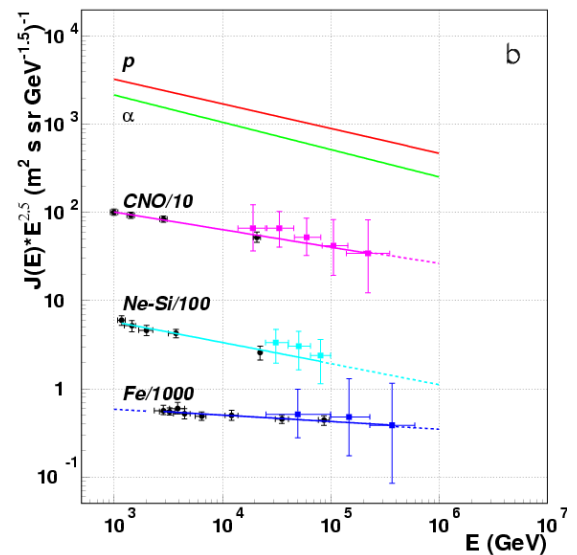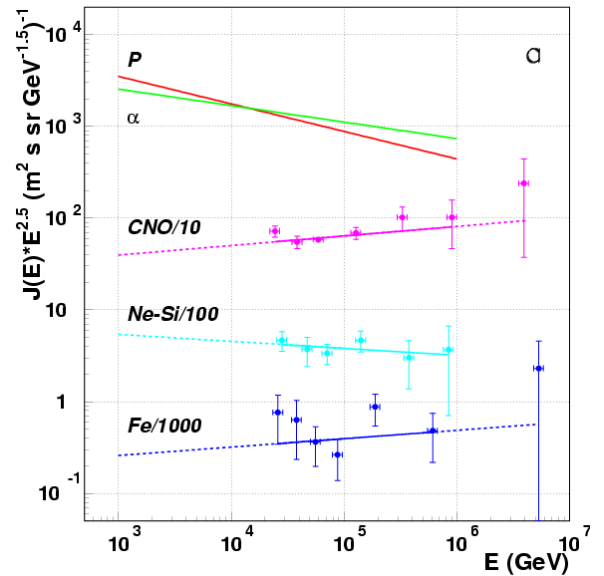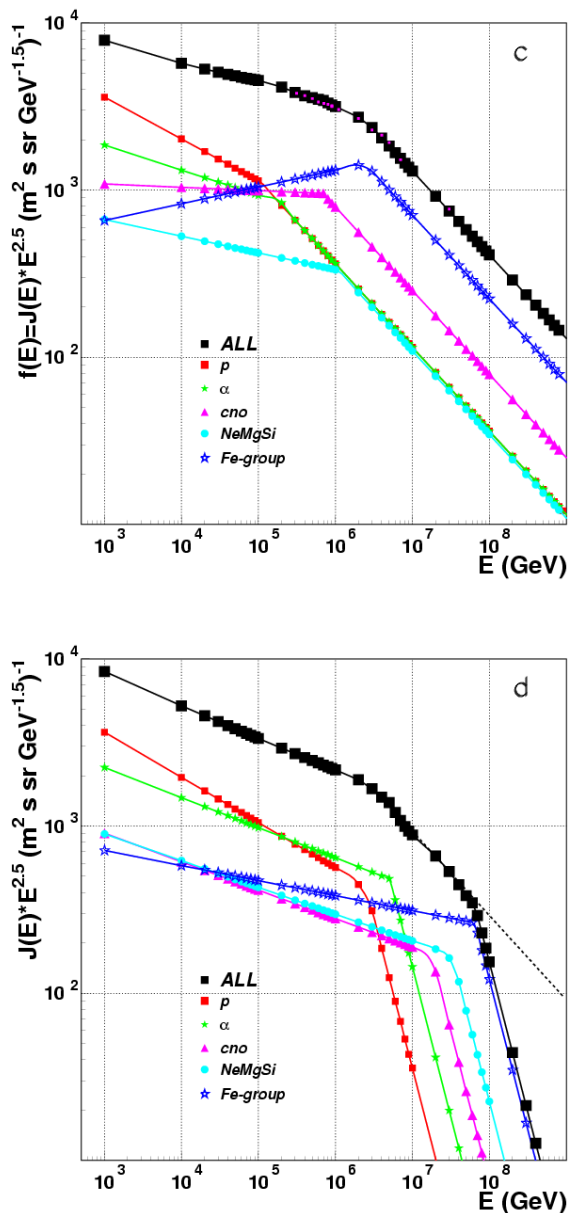
Fig. 3. Composition models: a) JACEE; b) RUNJOB; c) TIBET ASγ; d) Horandel.

The RUNJOB model is shown in Fig. 3b. The data are in the 10÷500 TeV range. No structure is seen in the spectra. For protons and alphas the power law

behavior found by the collaboration is shown in figure, while the for the other components we did a single power law fit using the CRN [14] data at lower energies, as suggested by the RUNJOB collaboration itself.

A comparison between the two experiments reveals: a) a difference in the spectral index of the estimated *all particle spectrum*, namely 2.78 (RUNJOB) and 2.58 (JACEE ); b) the alpha spectra differ both in absolute value and spectral index, there is about a factor 2 between them; c) both experiments agree that there is no evidence for a break in the proton spectrum around 100 TeV.

The model used by TIBET ASγ to convert measured size to primary energy is the so called *Hadron-Dominant-Model* (HD). This composition model is inspired by the standard model of cosmic rays, it assumes a knee in the proton spectrum around 100 TeV and a knee at the same rigidity for the other components, moreover the iron contribution increases as the energy gets closer to the knee energy (Fig. 3c). The Tibet ASγ measurements are in  the $3 \cdot 10^2 \div 2 \cdot 10^4$ TeV range and  show a smooth change of the slope more than a sharp break in the all particle spectrum, the resulting knee is at about 2 PeV and would be caused by the iron contribution.

In the Horandel  model – Fig. 3d **-** the fluxes obtained by direct measurements are extrapolated to high energies and compared to the results of indirect measurements. The normalization point is at 100 TeV. According to theories for cosmic ray acceleration, the energy spectra of individual nuclei are assumed to follow power laws with a cut-off at high energies which depends on Z. Taking into account contributions from heavier nuclei and an "ad hoc" extragalactic component above 100 PeV, the model is able to consistently describe the measured all particle spectrum in the range from 10 GeV to almost 1 EeV. The observed knee would result from the proton spectrum bending at 1-2 PeV. The model has been recently updated.

## Calculation of $P_A(N_s, E)$ and $\varepsilon_A(E)$

The calculation of   $P_A(N_s, E)$ and $\varepsilon_A(N_s)$ has been done by Monte Carlo method [7]. $P_A(N_s, E)$ has been calculated by generating quasi-vertical ($\theta < 15°$) showers with core in a fiducial area $A_f$ of about 260 $m^2$ at the center of the carpet ($2 \times 3$ CLUSTERs)

with the CORSIKA/QGSjet code. Then the strip multiplicity distribution on the total carpet has been obtained. A detector efficiency of 95% and a strip multiplicity of 1.2 strip/particle were taken into account. According to expectations the logarithm of the strip multiplicity is log-normal distributed as shown in Fig. 4. Therefore, defining $y_s = \log_{10}( N_s )$, the formula for $P_A(y_s, E)$ results in

$$P_A(E, y_s) \equiv \frac{1}{N_{evt}(y_s)} \left. \frac{dN_{evt}(y_s)}{dy_s} \right|_{A,E} = \frac{e^{-\frac{1}{2}\left[\frac{y_s - \bar{y}_s(A,E)}{\sigma_{y_s}(A,E)}\right]^2}}{\sqrt{2\pi}\sigma_{y_s}(A,E)}$$

where

$$\bar{y}_s(A,E) \qquad \text{and} \quad \sigma_{y_s}(A,E)$$

are the mean logarithm of the strip multiplicity and the variance of the $y_s$ distribution for a given mass number A and energy E.

Starting from distributions like those in Fig. 4 these two parameters have been extracted by fit. The $y_s(A,E)$ functions (Fig. 5) were obtained by interpolating the values at different energies with a fifth order polynomial in log (E); $\sigma_{ys}(A,E)$ was interpolated with a power law.

The following chain of conditions were applied in order to select events in the fiducial area, and therefore to calculate $\varepsilon_A(N_s)$:

1) events were generated with core in an area much wider than the carpet, 150 x 150 $m^2$;
2) events were triggered with at least 16 PADs fired in any of the 4 x 5 central CLUSTERs, the trigger area ($A_t$);
3) the reconstructed events had to be within 15° from the vertical;
4) the reconstructed core [15] had to be in a selection area ($A_s$) of 6 x 7 central CLUSTERs; the selection area contains the trigger area;
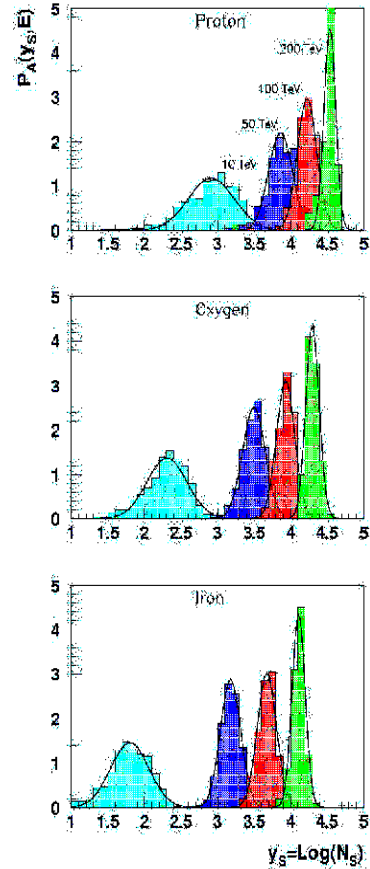5) finally, only events with core in $A_f$ were counted.



Fig. 4. The $y_s$ distributions to calculate $P_A(y_s, E)$.

The condition 2) – trigger condition - reflects the fact that proton showers start to have a defined core at about 10 TeV and that the mean particle density at the core position is about 0.5-1 particle/$m^2$. The corresponding trigger rate is < 10 Hz/cluster according to the results of ARGO-Test [16]. The condition 4) guarantees that events with core at the border of $A_t$ are also taken.

The efficiency $\varepsilon_A(N_s)$, see Fig. 6, represents the fraction of triggered and reconstructed events with core in $A_f$. The energy threshold, defined as the energy corresponding to 50% efficiency, is about 7 TeV for protons and 30 TeV for iron.

## 4. Results

The result of the calculation is shown in Fig. 7 where the function

$$F_{all}(y_s) = J_{all}(y_s) \cdot 10^{1.5\, y_s} \cdot \Gamma \cdot \Delta y_s$$

is reported.
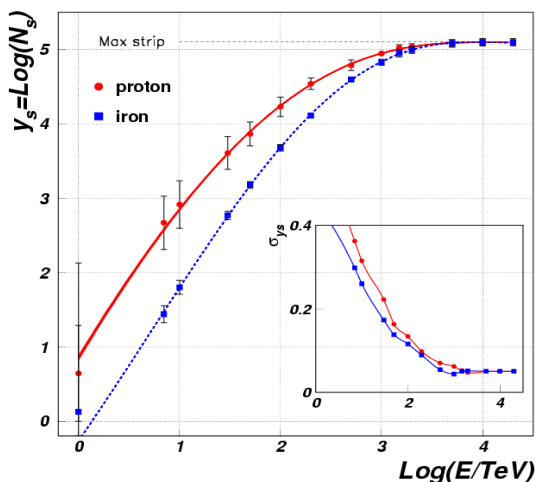


Fig. 5. Mean value and variance of $y_s$ as function of the energy for proton and iron initiated showers.

$F_{all}(y_s)$ provides the counting of strip multiplicity in a certain $\Delta y_s$ bin for a given exposure $\Gamma$, at the above trigger conditions. $\Delta y_s$ is taken equal to 0.1 and $\Gamma$ equal to $10^8$ $m^2$ s sr, corresponding to about 1 month of data taking.

This function provides in a simple way the slope of the strip size spectrum ($J_{all}(y_s) = C\, N_s^{-\alpha s}$); for reference we report in Tab. 1 the indices of the differential distributions obtained from Fig. 7. Moreover in Tab. 1 we report the expected counts in the $y_s$ bin centered at 3.5 ($\Delta y_s = 0.1$).

| JACEE | RUNJOB | TIBET ASγ | Horandel |
|---|---|---|---|
| Spectral Index | | | |
| 2.30 | 2.37 | 2.27 | 2.32 |
| Counts | ($<y_s>$=3.5, $\Delta y$=0.1 e $\Gamma$=$10^8$ $m^2$ s sr) | | |
| 18000 | 15336 | 20390 | 18544 |

Tab 1. Spectral indices of the strip multiplicity distribution and relative counts in a $y_s$ bin for the considered models (see text).

The $F_{light}$ distribution, calculated by considering just the light component contribution (protons + alphas), is shown in Fig. 8.

Fig.7 allows the following considerations:

1. for the given trigger setup and the considered geometry, the strip size multiplicity $y_s$ ranges from 3.1 to 4.2 without any limitation in the spectrum. Above this range the saturation starts ($<E_p> > 100$ TeV, $<E_{Fe}> > 250$ TeV), while below the spectrum
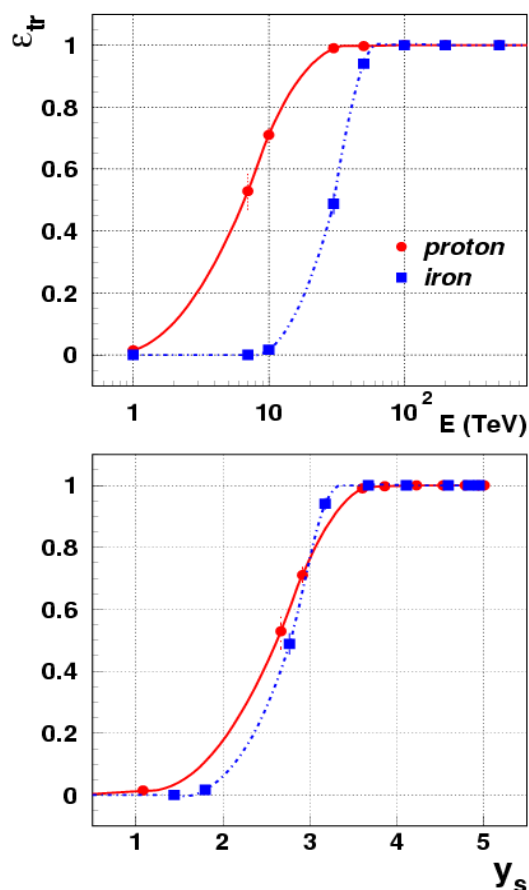




Fig. 6. The trigger efficiency $\varepsilon_A(N_s)$ for proton and iron induced air showers.

shows the effect of the trigger inefficiency (at 90% efficiency $<E_p>$ =15 TeV and $<E_{Fe}>$ = 40 TeV );

2. in the $y_s$ range $3 \div 4$ the JACEE model and the Horandel model predict almost the same spectrum with $\alpha_s = 2.30$ and $2.32$ respectively. The biggest difference is found between the predictions of the TIBET AS$\gamma$ and the RUNJOB models, the spectral indices being 2.27 and 2.37 respectively;

3. for the considered exposure( $\Gamma = 10^8$ m$^2$ s sr), the number of events in each size bin is enough to make negligible the statistical uncertainty; on the other hand, any systematic error $\delta N_s / N_s$ in reconstructing the strip size spectrum determines an error $\delta F_{all} / F_{all}$ $= (\delta N_s / N_s + 1)^{\alpha s - 1}$. Therefore a control on the detector performance at a level better than 10% is required in order to reduce any systematic effect below 15%.

Looking at the light component, Fig. 8 shows that it is impossible to distinguish among the JACEE, RUNJOB and Horandel models, instead the
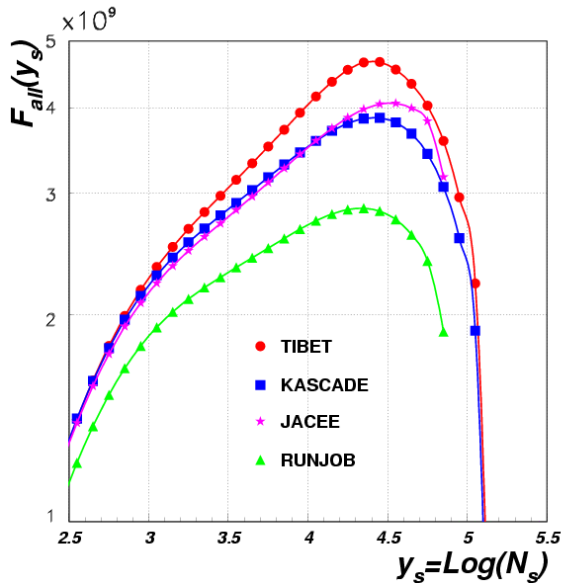


Fig. 7. Strip size spectrum resulting from the considered models of primary composition (see text).

TIBETAS$\gamma$ model predictions are quite different and can be checked against the other ones.

Both figures do not show any sensitivity to the knee position.

## 5. Conclusions

The possibility of discriminating between different models of primary cosmic ray composition by using

the digital read-out of ARGO-YBJ has been investigated. It is important to notice that this technique should allow to scan the energy range from 10 to a few hundreds of TeV where direct and indirect measurements partially overlap.

The proposed measurement procedure is simple to implement, it requires just a density trigger in a central area of the detector; no calibration is needed while a stable detector behavior is certainly fundamental.

It results that ARGO-YBJ has a fairly good sensitivity to discriminate between different composition models, provided that systematic uncertainties are kept below 10%. Among the models considered, TIBET and RUNJOB can be resolved ; the JACEE and Horandel models cannot be, moreover they are only partially resolvable with respect to any of the other two.

There is no sensitivity to the knee position even in case the light component could be isolated.
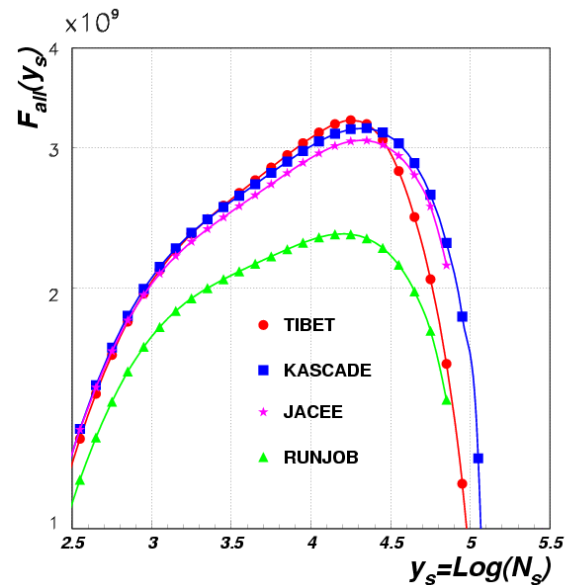


Fig. 8. Strip size spectrum resulting from the considered models of primary composition, taking into account only the light component (protons + alphas).

## References

[1]  Horandel J.R., Astropart. Phys. 21 (2004) 241.

[2] Amenomori M. et al., Phys. Rev. D, 62,112001-1 (2001).

[3] Antoni T. et al., Astropart. Phys.16, 373 (2002).

[4] Apanasenko A.V. et al., Astropart. Phys.16,13 (2001).

[5] Surdo A. et al., proc. 28th ICRC ( Tsukuba) 1, 5 (2003); Abbrescia M. et al., Astroparticle Physics with ARGO, Proposal (available at http://argo.na.infn.it)

[6] Bacci C. et al., NIM A 443, 342 (2000).

[7] Saggese L., PhD Thesis, Università di Napoli (2002) – unpublished; Saggese L. et al., proc. 28th ICRC (Tsukuba) 1, 263 (2003).

[8] Knapp J. et al., Forschungszentrum Karlsruhe FZKA 6019 (1998).

[9] Iacovacci M. et al., proc. 28th ICRC ( Tsukuba) 2, 757 (2003).

[10] Asakimori K. et al., Astrophys. Journ. 502, 278 (1998).

[11] Horandel J.R. et al. 2001, proc. 27th ICRC (Hamburg) 1, 71; Horandel J.R, Astropart. Phys. 19, 193 (2003).

[12] Asakimori K. et al., proc. 23rd ICRC (Calgary) 2, 21 and 2, 25 (1993).

[13] Cherry M.L. et al., proc. 26th ICRC (Salt Lake City) 3, 187 (1999).

[14] Swordy S. P. et al., Astrophys. Journ. 403, 658 (1993).

[15] Di Sciascio G.et al., proc. 28th ICRC ( Tsukuba) 5, 3015 (2003); Martello D. et al., proc. 28th ICRC ( Tsukuba) 5, 3011 (2003).

[16] Bacci C. et al., Astropart. Phys. 17, 151 (2002).